

The origin of water-vapor rings in tropical cold pools

Wolfgang Langhans¹, David M. Romps^{1,2} (contact: wlanghans@lbl.gov)

¹Earth Sciences Division, Lawrence Berkeley National Laboratory, Berkeley, CA

²Department of Earth and Planetary Science, University of California, Berkeley, CA

INTRODUCTION AND MOTIVATION

Evaporatively driven cold pools over tropical oceans are known to “pre-condition” the PBL for a subsequent triggering of deep convection. A moist static energy excess in the PBL is associated with rings of enhanced water vapor content near cold pool edges (Tompkins 2001, Moeng et al. 2009).

Figure 1 illustrates the presence of such vapor rings in a simulation of radiative-convective equilibrium (RCE) (e.g., Jeevanjee and Romps, 2015). Also shown is the distribution of CAPE, which is tightly coupled to the near-surface water vapor distribution.

Tompkins (2001) suggested these vapor rings form from evaporatively moistened PBL air that gets laterally displaced by and entrained into the high-density downdraft air. However, a thorough analysis of these mechanism and of the actual origin of these vapor rings has not been carried out so far.

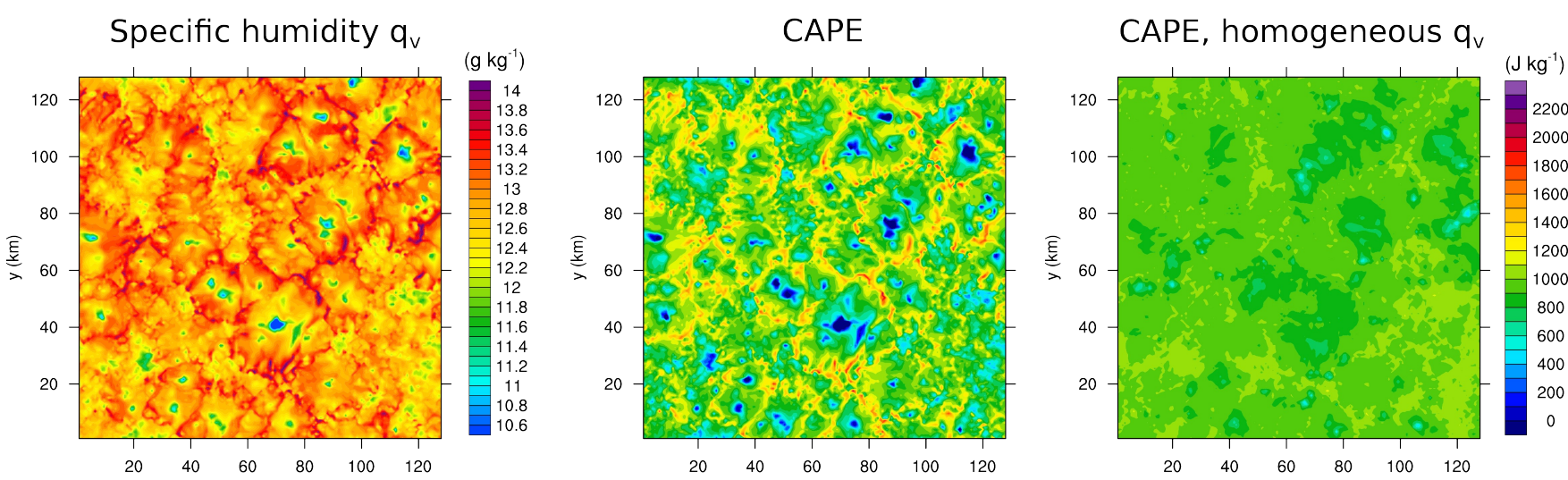


Figure 1. A typical RCE scenario illustrating the spatial heterogeneity due to cold pools. Shown are specific humidity in the boundary layer, convective available potential energy (CAPE), and CAPE computed from parcel ascents started with the same domain-mean specific humidity. The vapor rings are key to the destabilization of the atmosphere.

OBJECTIVES

- 1) What's the origin of water vapor rings in tropical cold pools?
- 2) What are the individual contributions from evaporation or rain, surface latent heat fluxes, and the pre-existing PBL moisture anomaly?
- 3) Are the underlying physics in line with the conceptual ideas proposed by Tompkins (2001)?

REFERENCES

- Jeevanjee, N. and D. M. Romps, 2015: Effective buoyancy, inertial pressure, and the mechanical forcing of deep convection by cold pools. *J. Atmos. Sci.*, submitted.
- Moeng, C.-H. and others: The tropical marine boundary layer under a deep convection system: a large-eddy simulation study. *J. Adv. Model. Earth Syst.*, **1**, 16.
- Romps, D. M., 2008: The Dry-Entropy Budget of a Moist Atmosphere. *J. Atmos. Sci.*, **65**, 3779–3799.
- Tompkins, A. M., 2001: Organization of tropical convection in low vertical wind shears: The role of cold pools. *J. Atmos. Sci.*, **58**, 1650–1672.

ACKNOWLEDGMENTS

This work was supported by the U.S. Department of Energy’s Atmospheric System Research, an Office of Science, Office of Biological and Environmental Research program under Contract No. DE-AC02-05CH11231. This research used computing resources of the National Energy Research Scientific Computing Center (NERSC), which is supported by the Office of Science of the U.S. Department of Energy under Contract DE-AC02-05CH11231, and computing resources of the Extreme Science and Engineering Discovery Environment (XSEDE), which is supported by National Science Foundation Grant OCI-1053575.

Large-eddy simulations of quasi-axisymmetric cold pools

“Das Atmosphärische Modell” DAM (Romps, 2008)

- Domain: $20 \times 20 \times 14.1 \text{ km}^3$ double-periodic, horizontal grid-spacing $\Delta x = 50 \text{ m}$, vertically stretched grid with $\Delta z = 10 \text{ m}$ in lowest 400 m

Warm-bubble simulation

- Atmosphere at rest with RCE thermodynamic profiles; cumulus cloud initiated by a 1-K near-surface temperature perturbation (“half-dome” with radius=1 km)
- Additional vapor perturbation ($\Delta q_v = 1 \text{ g kg}^{-1}$, radius=3 km) to mimic pre-existing PBL moisture anomaly

Water vapor mass tracers

- Four tracers are evolved to distinguish vapor mass from different origins (see Table 1)
- Tracers are initialized right before onset of rainfall at time $t_r \approx 1000 \text{ sec}$
- A base state q_{base} with horizontally homogeneous q_v below cloud base is defined at time t_r

Tracer mass fraction	q_{base}	q'_{pbl}	q'_{lh}	q'_{er}
Meaning	Base state (homog. PBL before rainfall)	Pre-existing PBL perturbation	Pert. due to rain evaporation	Pert. due to surface latent heat flux
Initialization at t_r	q_{base} (see caption)	$q_v - q_{\text{base}}$	0	0
Mass source	0	0	Rain evaporation	Surface latent heat flux

Table 1. Summary of attributes of four different water vapor mass tracers. The base state q_{base} is defined at t_r as $q_{\text{base}}(x, y, z, t_r) = \gamma(z)q_v(x, y, z, t_r) + [1 - \gamma(z)]q_v^*(z)$ with $\gamma(z) = 0.5 + 0.5\tanh[0.02(z - 500 \text{ m})]$ and q_v^* the profile of the unperturbed far-field.

VAPOR MASS DECOMPOSITION ACCORDING TO ORIGIN

Horizontal distribution

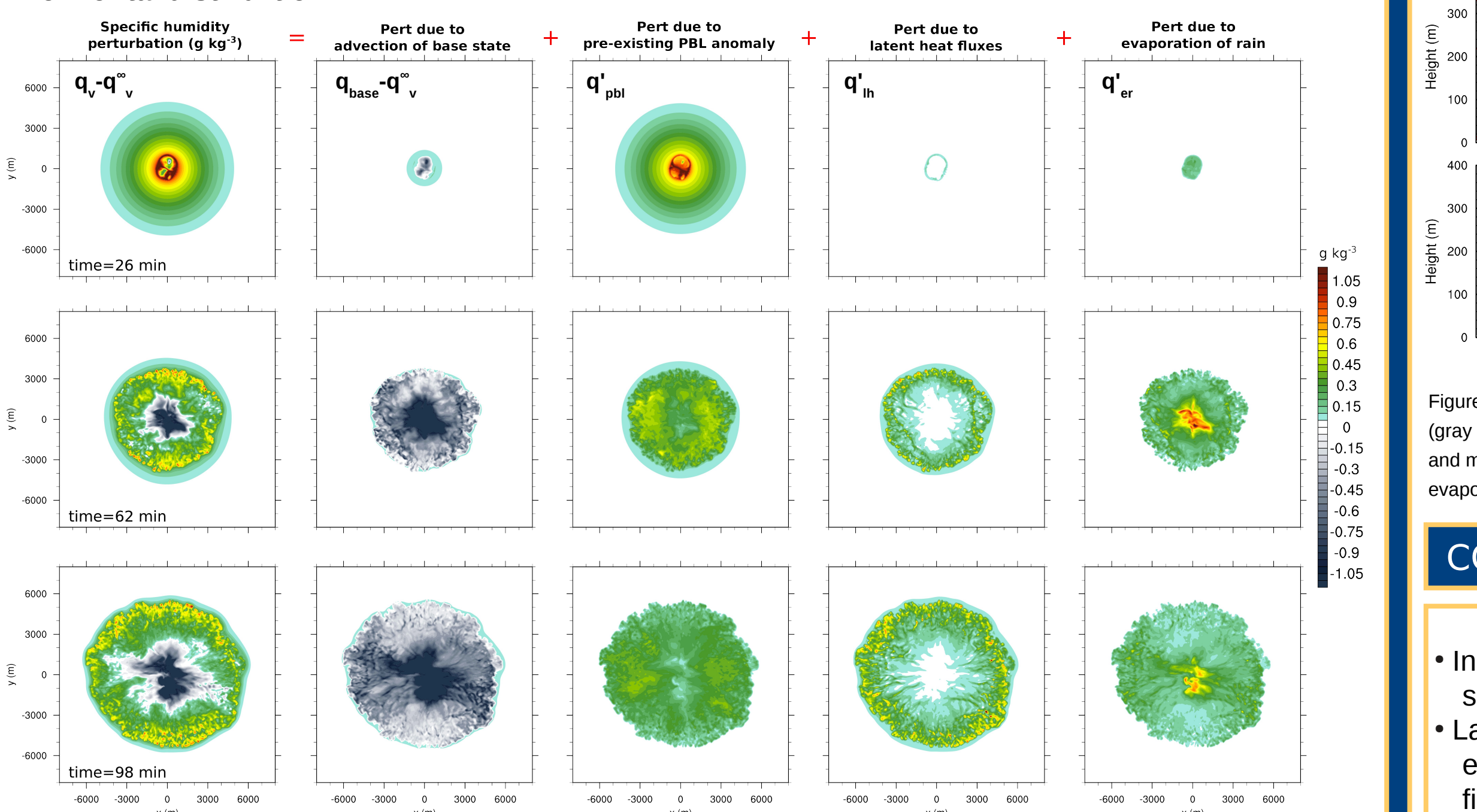


Figure 2. Decomposition of the perturbation water vapor mass fraction $q_v - q_v^*$ (1st column) into contributions from different origins. Distributions are shown after 26, 62, and 98 min. All quantities are computed as density-weighted vapor mass fractions for the lowest 100 meters. To obtain the perturbations in column 1 and 2, the far-field value q_v^* of the base-state vapor mass fraction has been subtracted. To very good approximation, the sum of the four rightmost panels yields the leftmost panel.

Vertical distribution

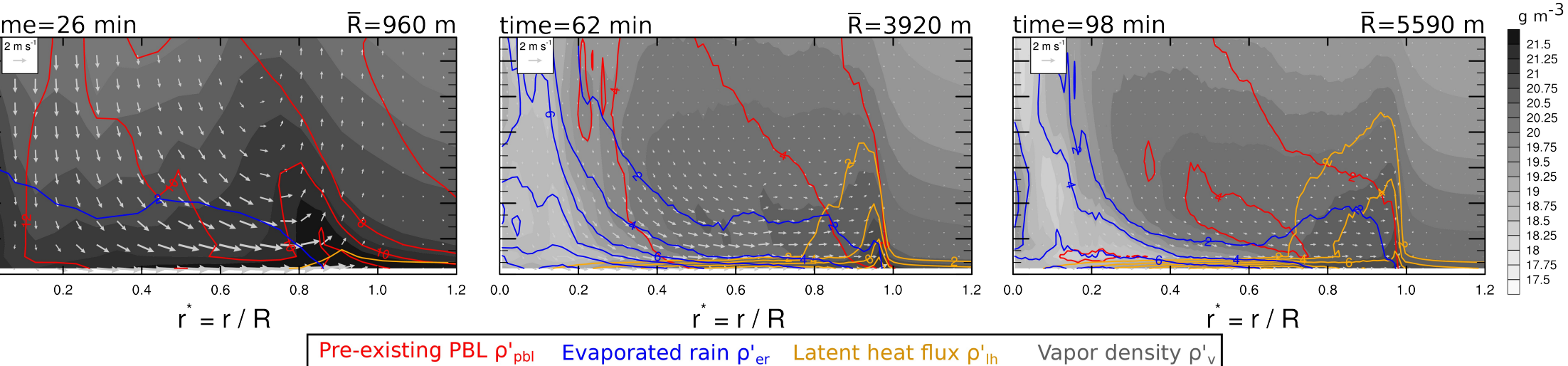


Figure 3. Azimuthally averaged r - z distributions of the water vapor density $p_v (\text{g m}^{-3})$, gray shading) and of the individual perturbations due to latent heat fluxes $p_{\text{lh}} = p q_{\text{lh}}$ (orange contours), due to evaporation of rain $p_{\text{er}} = p q_{\text{er}}$ (blue contours), and due to the pre-existing PBL vapor anomaly $p_{\text{pbl}} = p q_{\text{pbl}}$ (red contours) are shown after 26, 62, and 98 min. The three perturbations are contoured every 0.2 g m^{-3} (line labels are multiplied by 10). A normalized radial distance $r = r/R$ has been computed first for each grid column with R the radius at the leading edge. Averaging is then performed over r bins. The average R is indicated on top of each panel.

PBL PRE-MOISTENING BY EVAPORATING RAIN?

Necessary condition for validity of Tompkins' (2001) theory: sufficient evaporation of rain before onset of the divergent flow/downdraft.

Back-of-the-envelope estimate

- For an isobaric and adiabatic process the change in buoyancy B is $dB = -g d\ln p = -\frac{g}{1+r_t} dr_t + g \left(\frac{1}{\epsilon + r_t} - \frac{L_v}{C_p T} \right) dr_v$
- Instantaneous suspension of rain drops ($r_i = 5 \text{ g kg}^{-1}$) \Rightarrow Initial buoyancy $B_0 = -0.05 \text{ m s}^{-2}$
- For typical PBL values ($r = 18 \text{ g kg}^{-1}$, $T = 298 \text{ K}$): Evaporation rate of rain $E = 2 \times 10^{-6} \text{ s}^{-1} \Rightarrow dB/dt = -1.3 \times 10^{-4} \text{ m s}^{-3}$
- \Rightarrow Downdraft of $w = -2 \text{ m s}^{-1}$ is reached within only 40 sec due to hydrometeor drag
- \Rightarrow Evaporation of rain before lateral displacement of PBL air thus small: $\delta r_v = E \times 40 \text{ sec} = 0.08 \text{ g kg}^{-1}$

Confirmation by simulated onset of rainfall/downdraft

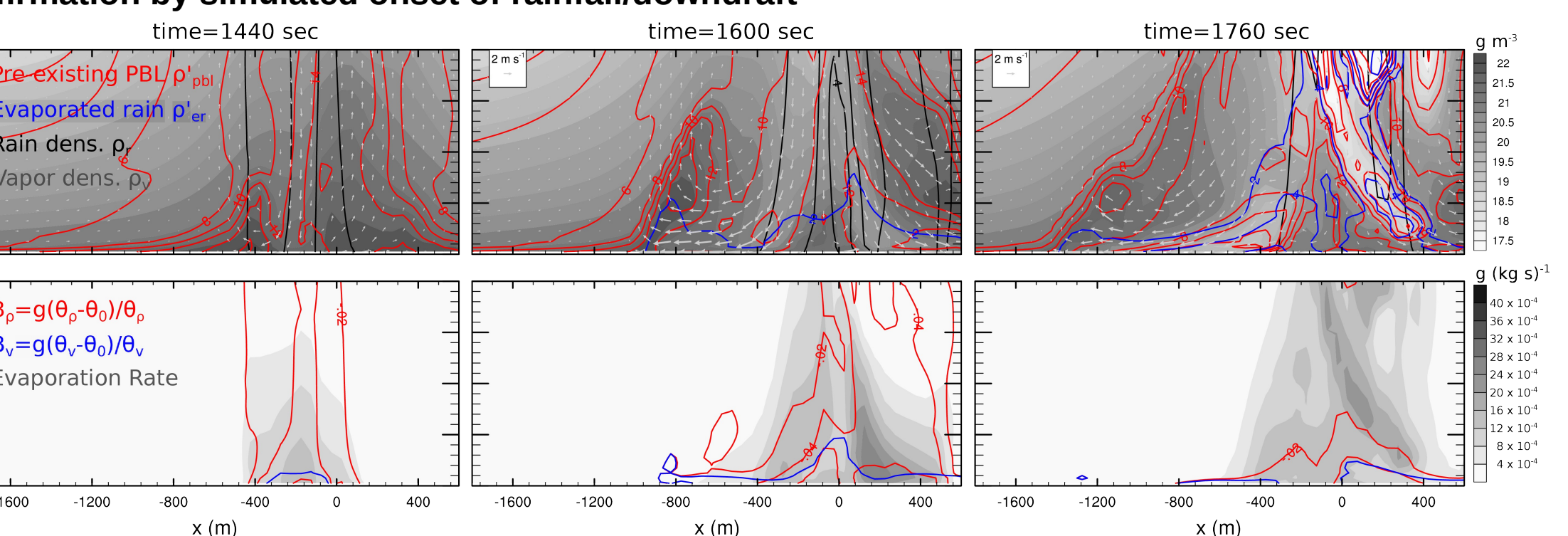


Figure 4. Vertical cross section illustrating the dynamics during the onset of rainfall after 1440, 1600, and 1760 sec. Top panels show the water vapor density p_v (gray shading) in g m^{-3} , velocity field (vectors), rain density $p_r = p q_r$ (black contours, every 2 g m^{-3}), pre-existing PBL moisture perturbation $p_{\text{pbl}} = p q_{\text{pbl}}$ (red contours) (both every 0.2 g m^{-3} , line labels are multiplied by 10). Bottom panels show the evaporation rate (gray shading) in s^{-1} and buoyancies B_v (blue) and B_p (red) every 0.02 m s^{-2} . Only B_p accounts for the weight of condensed water.

CONCLUSIONS

- In contrast to Tompkins' hypothesis, evaporation of rain is small before the onset of the downdraft
- Laterally displaced PBL air is relatively moist due to the pre-existing vapor excess which supported deep convection in the first place
- Vapor rings are “fed” by surface latent heat fluxes while cold pool propagates over the ocean

